

***XMM-Newton* Observations of the Cataclysmic Variable GW Lib**

Eric J. Hilton, Paula Szkody, Anjum Mukadam

Astronomy Department, Box 351580, University of Washington, Seattle WA 98115

`hilton@astro.washington.edu`

Koji Mukai

NASA/Goddard Space Flight Center, Greenbelt, MD 20771

Coel Hellier and Liza van Zyl

Astrophysics Group, Keele University, Keele, Staffordshire ST5 5BG, UK

Lee Homer

Liverpool CC, Liverpool, UK

ABSTRACT

XMM-Newton observations of the accreting, pulsating white dwarf in the quiescent dwarf nova GW Librae were conducted to determine if the non-radial pulsations present in previous UV and optical data affect the X-ray emission. The non-radial pulsations are evident in the simultaneous Optical Monitor data but are not detected in X-ray with an upper limit on the pulsation amplitude of 0.092 mags. The best fits to the X-ray spectrum are with a low temperature diffuse gas model or a multi-temperature cooling flow model, with a strong OVIII line, similar to other short period dwarf novae, but with a lower temperature range than evident in normal short period dwarf novae. The lack of pulsations and the spectrum likely indicate that the boundary layer does not extend to the surface of the white dwarf.

Subject headings: stars: individual – GW Lib – stars: dwarf novae – X-rays: stars

1. Introduction

GW Librae was the first cataclysmic variable in which the white dwarf was found to exhibit non-radial pulsations (Warner & van Zyl 1998). Since that first discovery, ten other

systems have been identified (see recent summary in Mukadam et al. (2007)), but GW Lib remains the brightest and best studied of the accreting, pulsating white dwarfs. It has a very short orbital period of 77 min (Szkody et al. 2000; Thorstensen et al. 2002) and a very low accretion rate, resulting in a large contribution of the white dwarf to the system light in the optical and ultraviolet regions of the spectrum. Parallax and proper motion measurements by Thorstensen (2003) give a distance of 104 pc. Until recently, only one outburst of GW Lib was known (Maza & Gonzalez 1983) but in April 2007, a second outburst began. Monitoring of the superhumps that developed during the course of the outburst (Kato 2007) revealed a period excess of the superhump period over that of the orbital period of 1.1%. The relation of period excess to mass ratio and orbital period (Patterson 2001) then implies that the secondary in GW Lib has passed the period minimum for close binary evolution and is degenerate.

Photometry over several years has shown the characteristics of the pulsations of GW Lib (van Zyl et al. 2004). There are three primary pulsation periods, although these all show different amplitudes at different times and some of the periods are not always visible. The most common periods are near 650, 370 and 230 s with typical amplitudes of 0.15, 0.010 and 0.007 mags. Woudt & Warner (2002) also identified a long period of 2.09 hrs that was present in 2001 observations but not during 1997-1998. The origin of this period is unknown but these long periods are present in several short orbital period disk systems.

Analysis of HST ultraviolet data (Szkody et al. 2002a) showed the same pulsations were present in the UV as the optical, but the amplitudes were about six times larger. An unexpected result from the HST study was that the best model fit to the spectrum was with a two-temperature white dwarf, with a $T_{eff}=13,300K$ for 63% of the white dwarf surface and 17,100K for the remaining 37%. It was unclear whether the dual temperatures were a result of the boundary layer (where the fast moving layers of the inner disk meet the slower rotation of the white dwarf) providing accretion heating of the equatorial regions of the white dwarf, or due to the pulsations. Further UV studies of accreting pulsating white dwarfs (Szkody et al. 2007) have not shown this dual temperature structure.

While the soft X-ray emission from the stellar photosphere of the single hot white dwarf PG1159-036 is known to exhibit similar pulsations modes as the optical but with 20-30 times the optical amplitudes (Barstow et al. 1986), the interesting question is whether the non-radial pulsations affect the boundary layer where the X-rays are produced in CVs. In order for theoretical disk instability models to account for the long interoutburst timescales between dwarf novae outbursts such as in GW Lib, the accretion rate has to be very low, requiring very low viscosity and truncation of the inner accretion disk, possibly by coronal siphons or from a strong magnetic field on the white dwarf (Meyer & Meyer-Hofmeister 1994;

Warner et al. 1996). Fitting of spectral energy distributions to models also often invokes a truncation of the inner disk in order to alleviate excess UV flux from the models (Linnell et al. 2007). If the inner disk of GW Lib is truncated, the X-ray emission should not be pulsed. However, *Chandra* data on the dwarf nova U Gem (Szkody et al. 2002b) shows that the boundary layer is close to the white dwarf and moving at low velocity. If the boundary layer in GW Lib extends to the white dwarf surface, the X-ray emission may be modulated at the same periods evident in the UV and optical. Thus, the X-ray emission from GW Lib could provide some constraints on the location and characteristics of the boundary layer in low accretion rate systems.

Since GW Lib was not detected in the ROSAT All Sky Survey, nor has any previous X-ray observation, we obtained time on *XMM-Newton* to obtain light curves and spectra to determine if GW Lib has the normal hard X-ray emission that is generally present in all low mass transfer rate, disk-accreting dwarf novae, and if the X-rays are modulated by the non-radial pulsations evident on its white dwarf.

2. Observations and Data Reduction

XMM-Newton observations of GW Lib on August 25-26, 2005 provided simultaneous optical imaging from the Optical Monitor (OM; Mason et al. 2001), and X-ray data from the EPIC pn (Strüder et al. 2001), and two MOS detectors (Turner et al. 2001). The pn has roughly twice the effective area of either MOS detector. Because of a low count rate, the Reflection Grating Spectrograph data were not useful. The X-ray observations lasted approximately 20ks, while the OM consisted of 5 observations of approximately 4ks each. The UT times, length of total observations, and average count rates are listed in Table 1.

The data were reduced using SAS (ver. 7.0.0) following the guidelines from the main *XMM-Newton* Web site (Vilspa) and from the NASA/GSFC XMM-Newton Guest Observer Facility ABC Guide (ver. 2.01). Calibration files are current to August 15, 2006. The SAS tools were used to create new event list files from the observation data files. In order to screen out background flaring events, whole-chip light curves for each detector were created in the 10-18 keV range and the data were ignored when the count rate was greater than 2.0 c/s for the pn and greater than 0.6 c/s for each MOS detector. These background flaring times when the count rate limits were exceeded were nearly identical for all detectors. The event list files were also screened with the standard canned expressions. The source aperture was taken to be circular with a radius of 360 pixels for the pn and 320 pixels for both MOS detectors in order to maximize the signal-to-noise. For the MOS detectors, the source-free background aperture was taken to be an annulus on the central chip centered on the source,

while for the pn the background was taken to be rectangular regions on adjacent chips with similar Y locations as the target. Energies were restricted to the well-calibrated ranges: 0.2 - 15 keV for spectral analysis and 0.1 - 12.5 keV for light curve analysis. Events were restricted for the pn to singles (pattern = 0) for the spectrum and singles and doubles (pattern ≤ 4) for the lightcurve. For the MOS detectors, up to quadruples (pattern ≤ 12) were permitted for both the spectrum and the lightcurve. FTOOLS¹ (Blackburn 1995) software tasks were used to group the spectral bins and associate various files for spectral analysis in XSPEC, create background subtracted light curves, and correct the time stamps to the solar system barycenter.

Data from both MOS detectors and the pn were combined to construct the X-ray light curve, which had an average count rate of 0.042 c/s. Only data when all three detectors were live and free of background flaring events were kept. These are called good time intervals. Data were also binned to increase the signal-to-noise of this faint source. The time bin size was chosen to be 150 seconds to simultaneously optimize signal-to-noise with time resolution. Although the time bins were primarily 150 seconds, the time bins at the edges of the good time intervals were of different sizes to accommodate all the data. The time bin size is discussed further in section 3.1.2.

For the OM observations, the B filter was used, and the Pipeline light curves were binned at 50 seconds for the analysis. The average count rate for the OM is 6.2 c/s, which is equivalent to a B magnitude of 17.3.

3. Results

3.1. Light Curves

3.1.1. Optical

The optical light curve of GW Lib, shown in Figure 1, is dominated by the 2.09 hour period that was intermittently present in the data of Woudt & Warner (2002). The discrete Fourier transform (DFT) of the optical data shown in Figure 2 shows this long period as well as modulations at 671 seconds with an amplitude of 0.02 mags and 397 seconds with an amplitude of 0.021 mags. These modulations are consistent with the previously observed pulsation periods near 650 s (1540 μ Hz) and 370 s (2700 μ Hz), whose periods and amplitudes are known to vary (van Zyl et al. 2004). Van Zyl et al. also find a pulsation near 230 s (4350

¹<http://heasarc.gsfc.nasa.gov/ftools/>

μHz) that is not seen in the OM data. However, the typical amplitude of this period is below the average noise level of this DFT, so its presence cannot be ruled out.

3.1.2. *X-ray*

The DFT of the combined X-ray data showed no significant periodicities. In order to place an upper-limit on the magnitude of variability, the following light-curve shuffling technique was applied to empirically determine the noise in the light curve. A light curve consists of a series of fractional intensity values each with a corresponding time value. Each value of fractional intensity was randomly reassigned to one of the unchanged, existing time values. This random shuffling destroys any coherent frequencies in the light curve but maintains the same time sampling and random white noise as the original light curve. The DFT of the shuffled light curve gives the amplitude of the noise at each frequency up to the Nyquist frequency. The original light curve was randomly shuffled 10 times and the average noise was computed each time. The noise of the original light curve was taken to be the mean of these 10 values.

As a check on the time bin size, light curves were produced with time bins of primarily 50, 75, 100, 150, and 200 seconds. In all cases, there were no strong signals present in the light curves and there were no significant differences in the average noise values. Because the count rate was so low, the time bin size was chosen to maximize the signal-to-noise without destroying the time resolution. Since the shortest period seen in the simultaneous optical observations was 397 seconds, the 150 second time resolution provides more than two points per cycle, which is sufficient time resolution. The unshuffled DFT is shown in Figure 2. The average noise averaged over ten random shufflings is 0.092 mags, which is taken to be the upper limit of the X-ray pulsations for GW Lib.

3.2. Spectral Analysis

The extracted background-subtracted spectrum from the pn detector was binned at 10 counts per bin to facilitate the use of χ^2 statistics to find the best fit models. The spectrum was restricted to the energy range 0.2-15.0 keV because the calibration of the EPIC detectors at the lowest energies is not certain and the count rate above 15.0 keV is too low to be useful. Although the data reduction allows high energy photons, there were very few photons detected with energies greater than 3 keV. The spectrum has a strong O VIII emission line at ~ 0.65 keV and an increase in emission at ~ 1.0 keV that is possibly

a Ne-Fe emission complex. Several models were used, starting with the simplest emission mechanisms (bremsstrahlung), and advancing in complexity to more detailed models and variable abundances. All models used absorption, but since all models consistently found a low value for the hydrogen column density, it was subsequently fixed at 10^{20} cm^{-2} to reduce the number of parameters. The redshift was fixed at 10^{-9} for the **mekal** and **mkcflow** families of models and the hydrogen density of the gas was fixed at 0.1 cm^{-3} for the **mekal** family of models. Parameters of the model and the goodness of fit statistics are listed in Table 2.

The simple absorbed bremsstrahlung (**wabs(bremss)**) model had a reduced $\chi^2 = 1.05$, but was unable to fit the strong emission lines. Explicitly adding a Gaussian to model the oxygen line decreased the residuals, and had a reduced $\chi^2 = 0.73$, but was unable to fit the lines near 1 keV.

The model of hot diffuse gas with line emissions from several elements **wabs(mekal)** with a solar abundance mixture also could not fit the emission lines (reduced $\chi^2 = 0.95$). The variable abundance version of this model (**wabs(vmekal)**) gave a better fit to the both the ~ 0.65 keV and the ~ 1.0 keV lines. All combinations of varying the oxygen, neon, and iron abundances were tried. As there were no significant differences in the model fits with different iron and neon abundances, these were finally left fixed at solar abundance. The model with oxygen as a parameter of the fit is shown in Figure 3, and has a reduced $\chi^2 = 0.81$.

Mukai et al. (2003) and Pandel et al. (2003) found successful fits using a cooling flow model (**wabs(mkcflow)**), so this model was also tried, although it did not fit the oxygen line nor fully fit the lines at ~ 1.0 keV. Adjusting the oxygen and neon abundances using (**wabs(vmcflow)**) did give a better fit to the emission lines with significantly higher oxygen abundance (compared to solar) and a slightly increased neon abundance. Since the mekal models showed that the neon abundance was very uncertain, the cooling flow model was also tried with leaving the neon fixed at solar abundance and allowing only the oxygen to be fit. This model is shown in Figure 4.

There are still residuals in both the vmekal and vmcflow model fits (Figures 3 and 4) near 0.9 keV. A Gaussian was added to the vmekal model at that energy but there was no significant improvement in the fits. Regardless of the model that was fit to the data, the temperature is generally low (1.5 - 2.5 keV) compared to most dwarf novae (Ramsay et al. 2001; Pandel et al. 2003; Hakala et al. 2004).

4. Discussion

The X-ray flux of GW Lib is much lower than expected for its optical magnitude and physical parameters. The cataclysmic variable WZ Sge has an orbital period and long-term outburst characteristics similar to GW Lib. The absolute visual magnitudes of the two systems are comparable (11.8 for WZ Sge and 11.9 for GW Lib) and the white dwarfs have comparable temperatures. Using the 4.5 keV thermal bremsstrahlung model of WZ Sge (Patterson et al. 1998) as a comparison, and correcting for distance, PIMMS predicts a count rate of about 0.1-0.2 c/s for GW Lib with the EPIC pn detector. The actual average count rate was much lower: 0.02 c/s for the pn and only 0.04 c/s after combining all three X-ray detectors (see Figure 1). *XMM-Newton* observations of other relatively nearby short period dwarf novae (T Leo, OY Car, VW Hyi, WX Hyi, SU UMa, TY PsA and YZ Cnc with orbital periods between 85-125 min and more frequent outbursts than GW Lib and WZ Sge), the pn count rates were between 1-7 c/s (Ramsay et al. 2001; Pandel et al. 2003; Hakala et al. 2004; Pandel et al. 2005). The 0.2-10 keV fluxes for the best fit vmekal (hot diffuse gas) and vmcflow (cooling flow) models for GW Lib shown in Figures 3 and 4 are 6.82×10^{-14} and 6.90×10^{-14} ergs cm $^{-2}$ s $^{-1}$ respectively. For a distance of 104 pc (Thorstensen 2003), the X-ray luminosity would be 9×10^{28} ergs s $^{-1}$. This compares to L_x of 4×10^{30} , 8×10^{30} and 1.4×10^{32} ergs s $^{-1}$ for OY Car, VW Hyi and YZ Cnc. Assuming this is the boundary layer luminosity, and using the relation given in Pandel et al. (2003):

$$L_{bl} = 5/2 \text{ kT}_{max} / \mu m_p$$

where T_{max} is the maximum temperature in the cooling flow model (5 keV), $\mu = 0.6$ and m_p is the proton mass, we can estimate that $\dot{M}_{bl} = 7 \times 10^{-14} M_{\odot} \text{ yr}^{-1}$. This value is typically 2 orders of magnitude lower than that for the other dwarf novae (Pandel et al. 2005). This value is also much lower than the time-averaged \dot{M} of 7.3×10^{-11} estimated by (Townesley et al. 2004) from their model parameters for GW Lib.

All model fits to the spectrum of GW Lib resulted in lower temperatures compared to OY Car, VW Hyi and YZ Cnc and the other systems as well. Although the best fit to all systems involve a range of temperatures, the maximum temperature for GW Lib is around 5 keV while the kT_{max} for the short period objects in Pandel et al. ranges from 8-26 keV. The low temperature is likely not due to an exceptionally low mass for the primary in GW Lib, as the UV fits (Szkody et al. 2002a) and the pulsation models (Townesley et al. 2004) indicate a high mass white dwarf. The low temperature in GW Lib suggests that the accreting gas is low density or is only mildly shocked, so the X-ray cooling is very inefficient. It is likely that the shock occurs high above the white dwarf surface which lowers the shock temperature. The stronger oxygen line in GW Lib compared to these other systems and the lack of FeK α at 6.4 keV are likely artifacts of the low temperature (although we cannot rule out that there

is some peculiar atomic physics that is not taken into account in the mekal-type models). It is noteworthy that FeK is also missing in WZ Sge and its temperature is similar to GW Lib (Patterson et al. 1998) so the lower accretion rates in these systems with rare but tremendous amplitude outbursts (Howell et al. 1995) likely lead to similar weak boundary layers.

The pulsations that are visible in the optical and UV are limited to an X-ray amplitude of < 0.09 mag. The low X-ray flux, cool temperatures and absence of strong X-ray pulsations all imply that the boundary layer in GW Lib does not reach to the white dwarf surface to create a strong shock or to be affected by the surface pulsations.

The lack of X-ray modulation at the 2.09 hr period argues against an origin for this period in the inner disk of a magnetic, precessing white dwarf as has been suggested for the long periods seen in FS Aur and HS2331+39 (Tovmassian et al. 2007).

5. Conclusions

The *XMM-Newton* observations of GW Lib have shown that the X-ray emitting region of the accreting, pulsating white dwarf is not strongly affected by the non-radial pulsations evident in the UV and optical. The unusually weak X-ray flux from this system precludes a stringent limit, but does rule out pulsation amplitudes of greater than 0.09 mag, specifically at the periods where significant signals are detected simultaneously in the optical band. The low X-ray flux, cool maximum temperature of the X-ray spectrum, combined with the lack of X-ray pulsation indicate the boundary layer is not dense enough to create a strong shock at the white dwarf surface. This has implications for the two-temperature model for the white dwarf that was needed to explain the HST UV spectrum (Szkody et al. 2002a) in that the origin of the hotter temperature component may be related to the pulsations, and not to boundary layer heating.

This work was supported by *XMM-Newton* grant NNG05GR47G to the University of Washington and is based on observations obtained with *XMM-Newton*, an ESA science mission with instruments and contributions directly funded by ESA Member States and the USA (NASA).

REFERENCES

Barstow, M. A., Holberg, J. B., Grauer, A. D., & Winget, D. E. 1986, ApJ, 306, L25

- Blackburn, J. K. 1995, in ASP Conf. Ser. 77: Astronomical Data Analysis Software and Systems IV, ed. R. A. Shaw, H. E. Payne, & J. J. E. Hayes (San Francisco: ASP), 367
- Hakala, P., Ramsay, G., Wheatley, P., Harlaftis, E. T., & Papadimitriou, C. 2004, *A&A*, 420, 273
- Howell, S. B., Szkody, P., & Cannizzo, J. K. 1995, *ApJ*, 439, 337
- Kato, T. 2007, vsnet-alert 9326
- Linnell, A. P., Hoard, D. W., Szkody, P., Long, K. S., Hubeny, I., Gänsicke, B., & Sion, E. M. 2007, *ApJ*, 654, 1036
- Mason, K. O. et al. 2001, *A&A*, 365, L36
- Maza, J., & Gonzalez, L. E. 1983, *IAU Circ.*, 3854, 2
- Meyer, F., & Meyer-Hofmeister, E. 1994, *A&A*, 288, 175
- Mukadam, A. et al. 2007, *ApJ*, Submitted
- Mukai, K., Kinkhabwala, A., Peterson, J. R., Kahn, S. M., & Paerels, F. 2003, *ApJ*, 586, L77
- Pandel, D., Córdova, F. A., & Howell, S. B. 2003, *MNRAS*, 346, 1231
- Pandel, D., Córdova, F. A., Mason, K. O., & Friedhorsky, W. C. 2005, *ApJ*, 626, 396
- Patterson, J., Richman, H., Kemp, J., & Mukai, K. 1998, *PASP*, 110, 403
- Patterson, J. 2001, *PASP*, 113, 736
- Ramsay, G. et al. 2001, *A&A*, 365, L294
- Strüder, L. et al. 2001, *A&A*, 365, L18
- Szkody, P., Desai, V., & Hoard, D. W. 2000, *AJ*, 119, 365
- Szkody, P., Gänsicke, B. T., Howell, S. B., & Sion, E. M. 2002a, *ApJ*, 575, L79
- Szkody, P., Nishikida, K., Raymond, J. C., Seth, A., Hoard, D. W., Long, K. S., & Sion, E. M. 2002b, *ApJ*, 574, 942
- Szkody, P. et al. 2007, *ApJ*, 658, 1188

- Thorstensen, J. R., Patterson, J., Kemp, J., & Vennes, S. 2002, *PASP*, 114, 1108
- Thorstensen, J. R. 2003, *AJ*, 126, 3017
- Tovmassian, G. H., Zharikov, S. V. & Neustroev, V. V. 2007, *ApJ*, 655, 466
- Townsley, D. M., Arras, P., & Bildsten, L. 2004, *ApJ*, 608, L105
- Turner, M. J. L. et al. 2001, *A&A*, 365, L27
- van Zyl, L. et al. 2004, *MNRAS*, 350, 307
- Warner, B., Livio, M., & Tout, C. A. 1996, *MNRAS*, 282, 735
- Warner, B., & van Zyl, L. 1998, in *IAU Symp. 185: New Eyes to See Inside the Sun and Stars*, ed. F.-L. Deubner, J. Christensen-Dalsgaard, & D. Kurtz (Dordrecht: Kluwer), 321
- Woudt, P. A., & Warner, B. 2002, *Ap&SS*, 282, 433

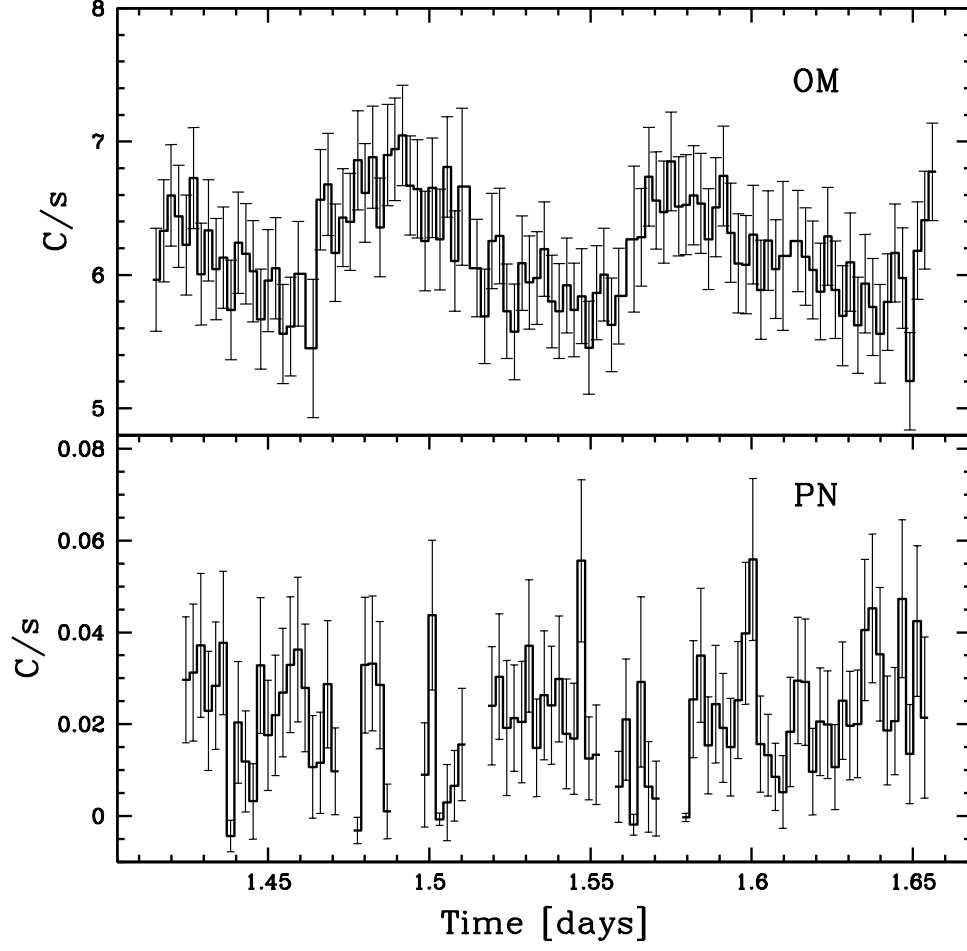


Fig. 1.— The optical lightcurve (top, shown here binned at 200 sec for clarity) shows a 2.09 hour period. The X-ray lightcurve (bottom) shows no apparent period. Notice the low count rate of the X-ray data.

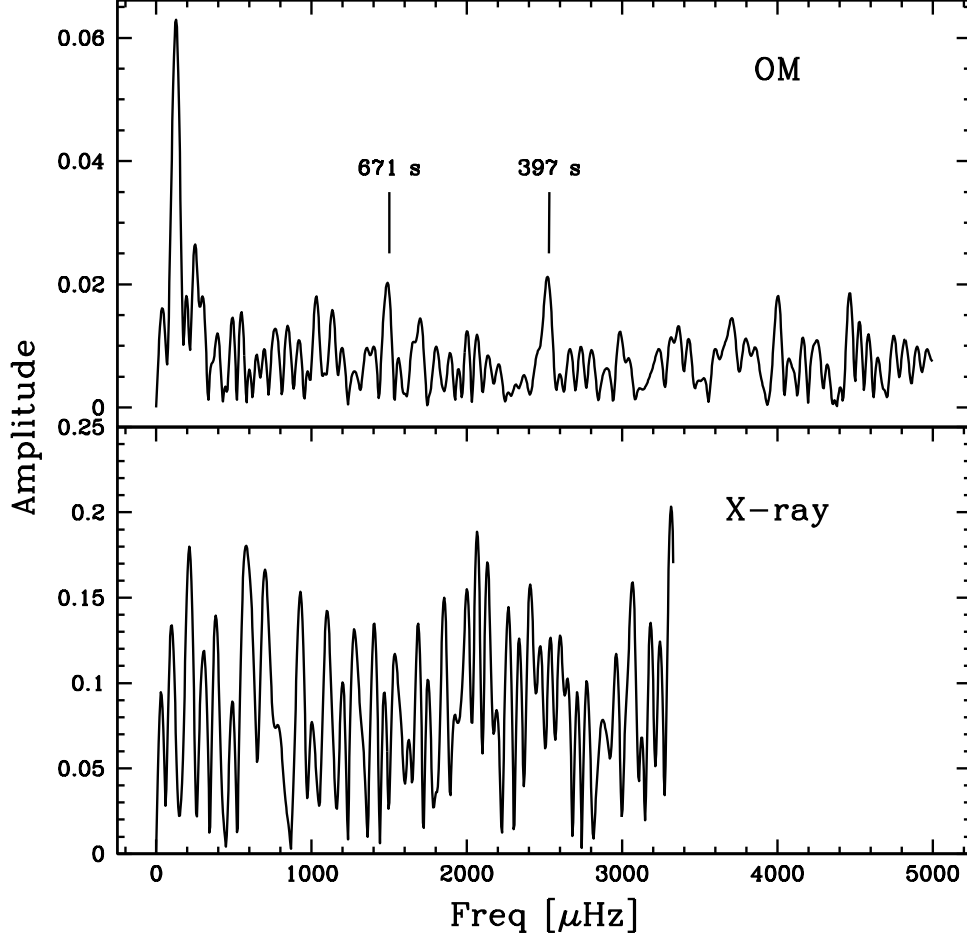


Fig. 2.— The DFT of the optical lightcurve binned at 50 sec (top) shows the 2.09 hour period as well as the two labelled periods from (van Zyl et al. 2004). The DFT of X-ray light curve binned at 150 sec (bottom) shows no periods. Note that with the longer time bins for the X-ray data, the Nyquist frequency is lower, and the DFT does not extend to as high frequencies as the OM data. See text for a discussion of the limit of variability.

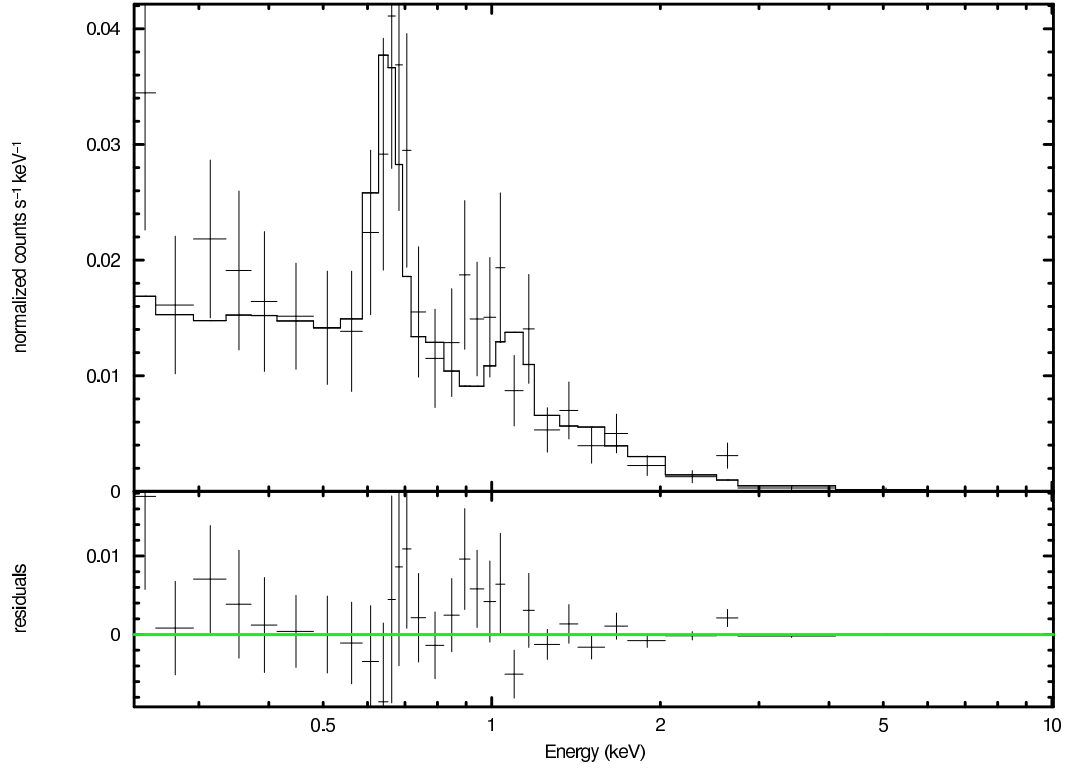


Fig. 3.— The hot diffuse gas model with variable oxygen abundance.

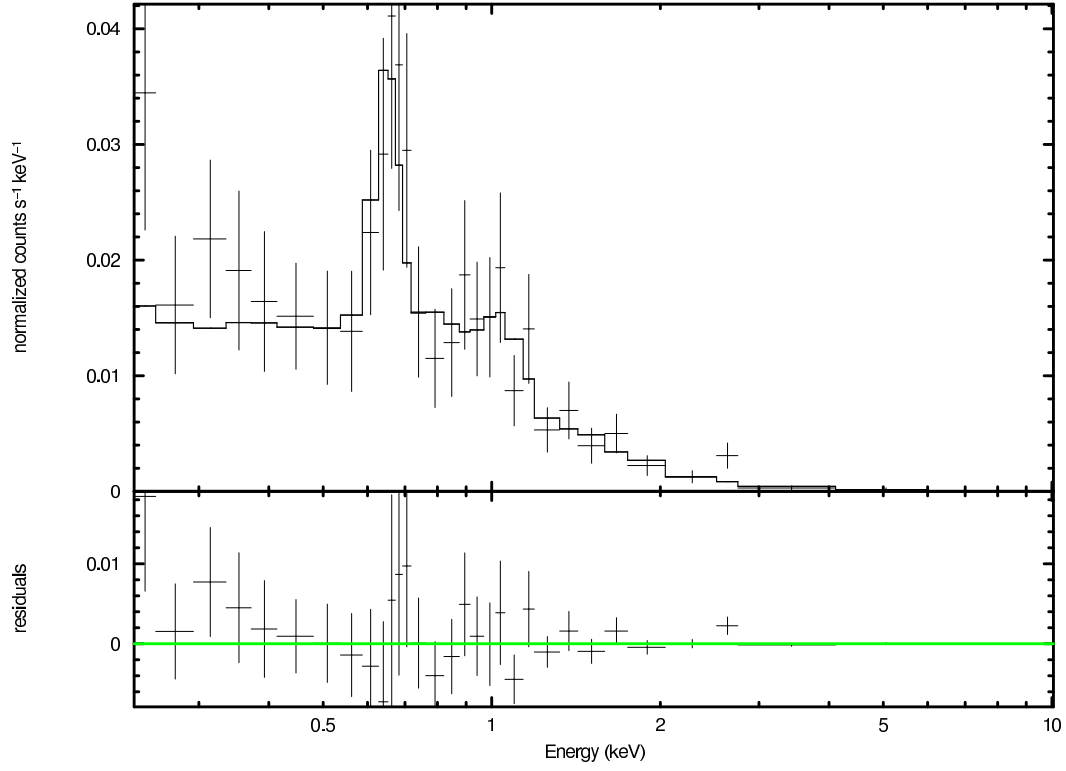


Fig. 4.— The cooling flow model with variable oxygen abundance.

Table 1. 25-26 August, 2005 Observations.

Instrument	Filter	Duration (s)	UT Start Time	UT Stop Time	Ave. count rate (C/s) ^a
PN	Thin1	19936	22:09:28	03:41:44	$(2.32 \pm 0.15) \times 10^{-2}$
MOS1	Thin1	21809	21:47:09	03:50:38	$(7.06 \pm 0.72) \times 10^{-3}$
MOS2	Thin1	21577	21:47:09	03:46:46	$(8.43 \pm 0.78) \times 10^{-3}$
OM	B	19901	21:55:31	03:48:49	6.2 ± 0.6 (B = 17.3) ^b

^aX-ray count rates determined from spectral reductions

^bOM count rate determined from light curve and converted to standard B magnitude

Table 2. XSPEC models used to fit the X-ray spectrum.

Model Name	Reduced χ^2	kT	Normalization	Parameters
Bremss ^a	1.05	2.2	2.3×10^{-5}	
Bremss ^b + Gauss	0.73	2.11	2.1×10^{-5}	LineE = 0.67 keV $\sigma = 9.9 \times 10^{-7}$ keV norm = 4.1×10^{-6}
mekal ^c	0.95	1.90	6.0×10^{-5}	abundance = 0.19
vmekal ^d	0.81	2.50	2.9×10^{-5}	O abund. = 7.99×solar
mkcflow ^e	0.83	0.091 - 4.70	1.6×10^{-16}	Abundance = 0.28
vmcflow ^f	0.70	0.38 - 5.52	1.4×10^{-16}	O abund. = 6.3×solar Ne abund. = 1.4×solar
vmcflow ^g	0.67	0.38 - 5.45	1.5×10^{-16}	O abund. = 6.12×solar

^aThermal Bremsstrahlung - Didn't fit the emission lines

^bThermal Bremsstrahlung plus Gaussian - Fit the oxygen line well

^cEmission from a hot diffuse gas - model shows bump at 0.6 keV, but doesn't fit line

^dEmission from a hot diffuse gas with variable abundances, neon fixed at solar

^eCooling flow

^fCooling flow with variable abundances

^gCooling flow with variable abundances, neon fixed at solar